A Virtual Impedance Based Grid Emulator for the Performance Analysis of Distributed Generations

Nakul Narayanan K and L Umanand
Department of Electronic Systems Engineering, Indian Institute of Science, Bangalore - 560012, India
Email: nakul@iisc.ac.in, lums@iisc.ac.in

***Abstract*—This paper presents a virtual impedance-based grid emulation technique to evaluate the performance of distributed generations connected to a grid/micro-grid. A two-level voltage source converter (VSC) with an output LC filter is used to emulate the grid. In the emulation, the grid is represented as a voltage source behind a virtual series impedance, where the impedance can be an inductor, a resistor, a capacitor or a combination of all the three. A simple estimator based active damping technique is proposed to damp out oscillations associated with the output LC filter of the VSC. A detailed time domain analysis is carried out in PSCAD/EMTDC to study the transient response of the emulator. A hardware prototype is developed to verify the performance of the emulator experimentally.**

I. Introduction

Distributed generations (DGs) are being integrated into the existing power network at different voltage levels to handle the increase in energy demand all over the world. At the distribution level, where the grid is weak (low short circuit capacity), the DG may be subjected to power quality issues like imbalance, sags and swells, harmonics and flicker at the point of common coupling (PCC) voltage [1]. Most of the DG resources are connected to the grid through current controlled VSC. The current controlled VSC faces stability issues when connected to a weak grid [2], [3]. Therefore, before connecting DG to the grid, it should be tested to ensure that it will operate in a stable way. In addition to this, power utilities demand DG to meet certain requirement specifications before connecting to their network, like low voltage ride through, dynamic voltage support capability, frequency ride through, anti-islanding functions etc. [4]. A high bandwidth grid emulator which can emulate all these scenarios, as well as the characteristics of a weak grid, can be utilized to test the DGs before commissioning.

Different methods to emulate the grid have been reported in the literature [5], [6], [7], [8]. Several commercial grid simulators are also available in the market [9], [10], [11]. In most of these, a VSC with an output LC filter is employed to emulate the grid. In [5], [8], a three-phase balanced simulator is developed with programmable voltage, frequency and harmonics. The control structure lacks in emulating voltage imbalance and series impedance. A grid simulator which can emulate balanced grid disturbance is discussed in [7]. Majority of the grid emulation techniques available emulates the grid as a voltage source without any series impedance and thereby cannot emulate a weak grid. In [12], an overview of virtual impedance-based control for voltage source converter and current source converter for grid connected applications is discussed in detail.

The LC filter connected to the output of the VSC to minimize switching frequency components causes resonance in the system. A simple way to damp these oscillations is to use a passive resistor in series or parallel with any of the filter elements. But this will result in power loss in the system. Active damping (AD) based techniques, where a virtual resistor is emulated in the control, can damp out the resonance without introducing additional losses in the system. Different methods to actively damp LC filter resonance have been reported [13], [14], [15], [16]. A Luenberger observer-based AD technique for LCL filter based on inverter current and the output voltage is proposed in [17]. Most methods use output capacitor voltage to estimate the capacitor current, which works well for grid-connected application or motor drives where the fundamental operating frequency is fixed and when the resonance frequency and fundamental frequency are well separated. In [13], the capacitor current at resonance frequency is calculated by integrating the capacitor voltage at the resonance frequency with proper scaling. In all these cases the operating frequency and the resonance frequency are well separated and the hence it is possible to filter out the resonance voltage. In a grid emulator, the output voltage needs to be regulated at the fundamental frequency as well as for harmonic frequencies. When the harmonic frequencies and resonance frequencies are not well separated, the above methods fail to estimate the capacitor current.

In this paper, a simple way to emulate a grid with a virtual series impedance is proposed. Any combination of resistor, inductor and capacitor can easily be emulated preserving their dynamic behaviour. The voltage controller is implemented in the stationary reference frame and can easily be extended to track higher order harmonic voltages. A simple estimator based active damping method is proposed to damp out the oscillations associated with the output LC filter. The rest of the paper is organised as follows. In section II, the basic idea behind grid emulation is discussed. The control structure and the proposed active damping is discussed in section III. Section IV discusses the controller design. Detailed time domain simulation and experimental results are discussed in section V. Finally, conclusions are drawn in section VI.

978-1-5386-8330-9/19/$31.00

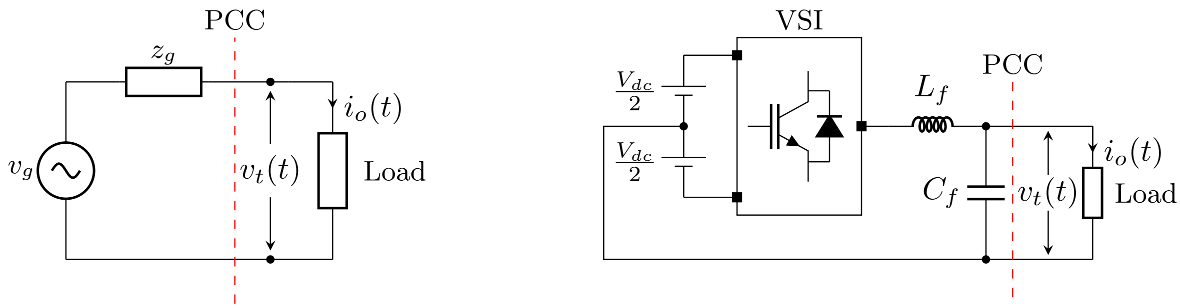

(a) Single phase representation of grid (b) Emulated grid

Fig. 1: Representation of inductor and capacitor

II. Grid Emulation

The grid can be represented as a voltage source behind a series impedance z_g as shown in Fig. 1a. Depending on load current i_o, the PCC voltage v_t changes. For example, if z_g is a series combination of R, L and C, then the PCC voltage $v_t(t)$ can be represented as follows,

$$v_t(t) = v_g(t) - \underbrace{\left[Ri_o(t) + L\frac{\mathrm{d}i_o(t)}{\mathrm{d}t} + \frac{1}{C}\int i_o(t)\mathrm{d}t \right]}_{v_d(t)} \quad (1)$$

The schematic of the grid emulator is shown in Fig. 1b. The terminal voltage $v_t(t)$ across the filter capacitor is controlled as per equation (1). If the load connected to the PCC is non-linear, then the terminal voltage $v_t(t)$ will contain harmonic voltage apart from the fundamental voltage. Depending on the nature of the grid, the impedance can be a simple inductor or a series-parallel combination of resistors, inductors and capacitors. The method to calculate voltage drop $v_d(t)$ in real time is discussed below.

A. Representation of Inductor and Capacitor

The passive elements inductor and capacitor are converted to Norton equivalent current source using Dommel's method [18], [19], by converting time-domain differential equations into a difference equation. For a time step of T_s, the inductor and capacitor can be represented as

1) Inductor: The relation between the voltage across and current through the discrete inductor given in Fig. 2a can be written as,

$$i_o(t) = \frac{1}{L}\int_{t-T_s}^{t} v_d(t)\,dt + i_o(t-T_s) \quad (2)$$

On applying trapezoidal rule,

$$i_o(t) = [v_d(t) + v_d(t-T_s)] \times \frac{Ts}{2L} + i_o(t-T_s) \quad (3)$$

The above equation can be written as,

$$v_d(t) = r_l \times (i_o(t) - I_{Lhys}) \quad (4)$$

where $r_l = \frac{2L}{T_s}$ and $I_{Lhys} = v(t-T_s)/r_l + i(t-T_s)$. From (4), inductor at a given instant 't', can be represented by a resistance r_l in parallel with a known current source I_{Lhys}.

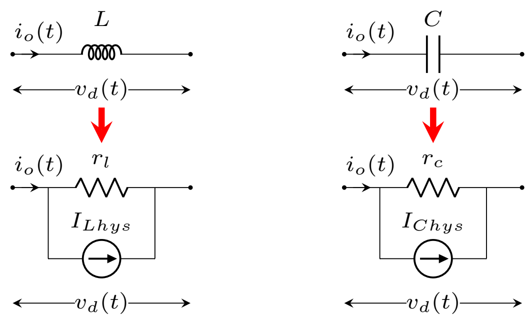

(a) Inductor (b) Capacitor

Fig. 2: Representation of L and C

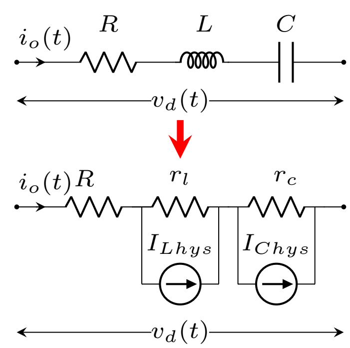

Fig. 3: Series RLC equivalent circuit

2) Capacitor: For the discrete capacitor given in Fig. 2b,

$$v_d(t) = \frac{1}{C}\int_{t-T_s}^{t} i_o(t)\,dt + v_d(t-T_s) \quad (5)$$

On applying trapezoidal rule,

$$v_d(t) = [i_o(t) + i_o(t-T_s)] \times \frac{T_s}{2C} + v_d(t-T_s) \quad (6)$$

The above equation can be written as,

$$v_d(t) = r_c \times (i_o(t) - I_{Chys}) \quad (7)$$

where $r_c = \frac{T_s}{2C}$ and $I_{Chys} = -[v(t-T_s)/r_c + i(t-T_s)]$. From (7), the capacitor at a given instant t, can be represented

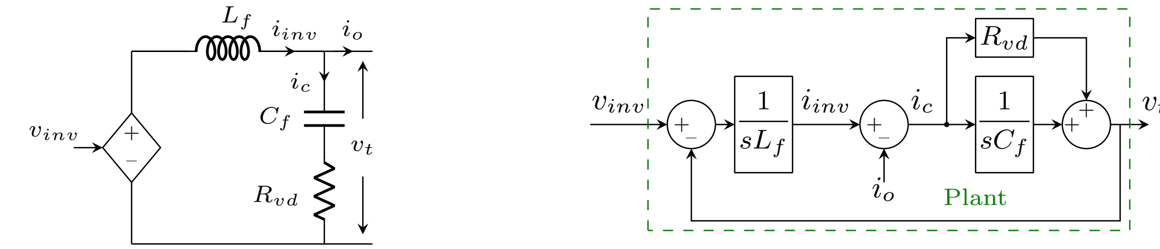

(a) Filter circuit

(b) Plant model

Fig. 4: With passive damping

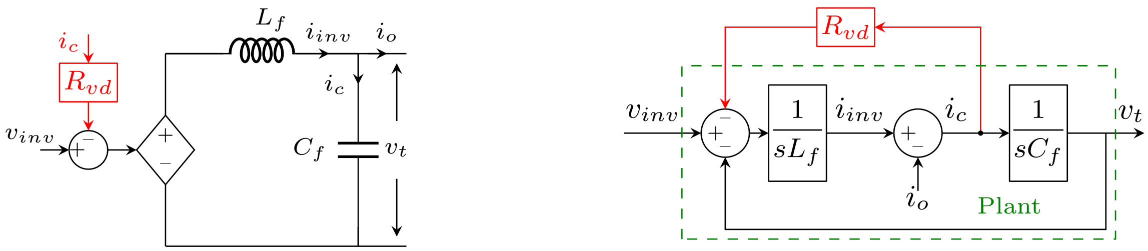

(a) Filter circuit

(b) Plant model

Fig. 5: With active damping

by a resistance rc in parallel with a known current source I_{Chys}.

Using (7) and (4) any series parallel combination of resistor, inductor and capacitor can be converted into equivalent current sources and resistor. The converted system can be solved with in one single time step. For example, the voltage drop across a series RLC impedance given in Fig. 3 can be written as,

$$v_d(t) = Ri_o(t) + r_c(i_o(t) - I_{Chys}) + r_l(i_o(t) - I_{Lhys}) \quad (8)$$

III. Control Structure

The grid emulator should be able to emulate virtual impedance, harmonic voltage, voltage imbalance, sag and swell etc. The control schematic of the grid emulator is given in Fig. 6.

A. Voltage Controller

The voltage drop v_d, across the virtual impedance is calculated by solving the network equation as discussed in section II to get the PCC reference voltage $v_t^*(t)$. If the load connected to the PCC is non-linear, then the terminal voltage $v_t(t)$ must be non-linear in nature. A proportional-resonant (PR) controller tuned at multiple frequencies is used to track PCC voltage with zero error [20]. The controller is converted to z-domain, and can be represented as,

$$G_c(z) = k_p + \sum_{h=1,3,5,7} \frac{a_{1h}z^{-1} - a_{2h}z^{-2}}{b_{0h} + b_{1h}z^{-1} + b_{2h}z^{-2}} \quad (9)$$

where h denotes harmonic order and $a_{1h}, a_{2h}, b_{0h}, b_{1h}, b_{2h}$ are coefficients of the controller for different frequencies [21]. In this work, harmonic resonant controllers are implemented for $h = 1, 3, 5\,\&\,7$.

B. Active Damping

The output of VSC is commonly connected through a low pass LC filter to reduce switching harmonics. This LC filter has a resonant frequency and if it is not properly damped, there will be an undamped oscillation at that frequency. There are several methods available in the literature to damp out these oscillations. Fig. 4a shows the circuit schematic of the LC filter with a physical damping resistor in series with the filter capacitor. The block diagram representation for this plant is shown in Fig. 4b. The above block diagram can be manipulated as shown in Fig. 5a to replace the physical damping resistor with a virtual damping resistor R_{vd}. The LC circuit with a virtual damping resistor will be as shown in Fig. 4a. To implement this active damping scheme, the capacitor current i_c needs to be measured. However, the capacitor current contains a considerable amount of switching frequency harmonic currents.

In this paper, the capacitor current i_c is calculated using an estimator. The structure of the proposed estimator-based AD is shown in Fig. 6. The inverter voltage, v_{inv} is estimated by multiplying the modulation index m with the average inverter model $G_{i,e}(z)$. The difference between the measured output voltage v_t and estimated inverter voltage v_{inv} is integrated using the integrator $G_{int}(z)$ with a time constant L_{fe}, (where L_{fe} is the estimated filter inductance) to calculate inverter current $i_{inv,e}$. The capacitor current $i_{c,e}$ is then estimated by subtracting $i_{inv,e}$ from measured load current i_o. The estimated capacitor current is multiplied by virtual resistance R_{vd} and scaled by converter gain ki (where $ki = \frac{2}{V_{dc}}$) and subtracted from the modulation signal $\widetilde{m}$ to implement active damping.

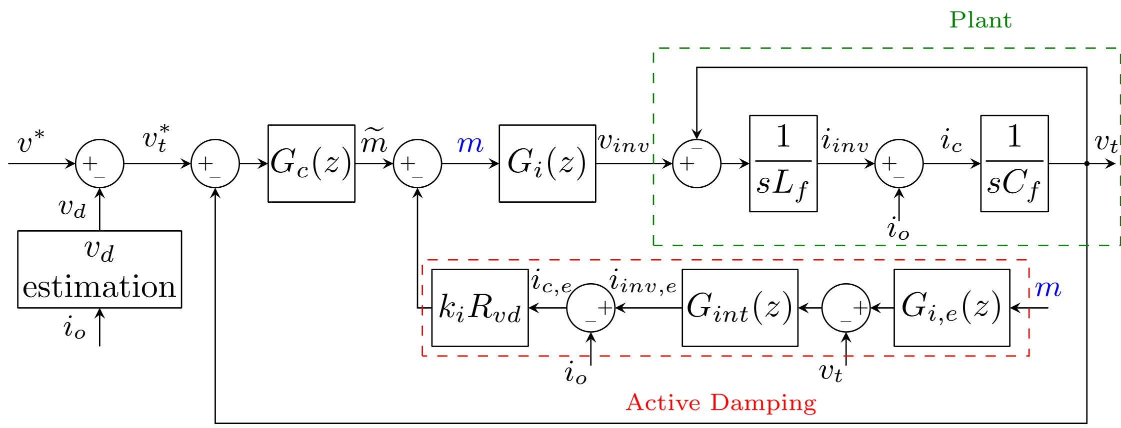

Fig. 6: Control schematic for one phase

C. Robustness of the proposed AD

The proposed active damping method depends mainly on the estimated inductor value L_{fe}. The control block given in Fig. 6 can be used to analyse the effect of the variation of the estimated inductance on the damping performance. The effective damping resistance ($R_{vd,e}$) seen by the system can be calculated as,

$$R_{vd,e} = R_{vd} \times \frac{L_f}{L_{fe}} \tag{10}$$

The difference between the estimated and actual filter inductance, results in a simple scaling of the virtual resistor. Considering a $\pm 10\%$ variation between the estimated and actual inductance value, the virtual resistor R_{vd} can be selected to provide enough damping for the entire range of variation.

IV. Controller Design

The design of the controller for the proposed grid emulator is performed in z-domain. The plant $G_p(s)$ in the continuous domain is converted into z-domain using zero-order-hold (ZOH) as given below.

$$G_p(z) = (1 - z^{-1})\mathbf{Z}\left[\frac{G_p(s)}{s}\right] \tag{11}$$

$$G_p(s) = \frac{1}{L_f C_f s^2 + 1} \; ; \omega_r = \frac{1}{\sqrt{L_f C_f}} \tag{12}$$

where w_r, is the resonance frequency of the LC filter. The inverter is modelled as a dc gain with a unit delay.

$$G_i(z) = \frac{V_{dc}}{2} z^{-1} \tag{13}$$

The open loop transfer function $G_{OL}(z)$ of the complete system can be derived from the above equations which can be used to design the controller for desired performance. In this paper the controller is designed to achieve a phase margin of 45°.

The bode plot of the open loop transfer function $G_{OL}(z)$ with and without active damping controller is plotted in Fig. 7. The LC filter resonance is well damped with the proposed active damping.

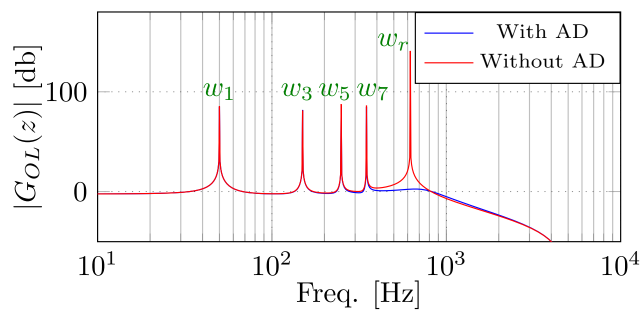

Fig. 7: Bode plot

V. Results

The performance of the proposed grid emulator is verified using detailed time domain simulation and experientially.

A. Time domain validation

To verify the dynamic performance of the grid emulator, a detailed time-domain simulation of the system given in Fig. 1b is carried out in PSCAD/EMTDC. For inverter, a detailed switching model is used. The VSC is rated at 400 V, 10 kVA and switched at 10 kHz ($T_s = 100\mu s$). The other parameters used in the simulation are: $L_f = 10$mH , $C_f = 5\mu$F. The load connected to the grid emulator is a resistive load. Fig. 8 shows the terminal voltage and load current for an inductive emulation of 100 mH. At $t = 2$ sec, a step change in load is

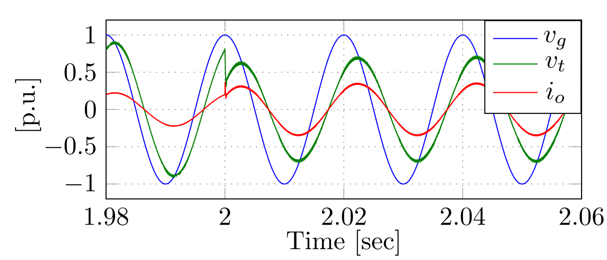

Fig. 8: Inductive impedance emulation

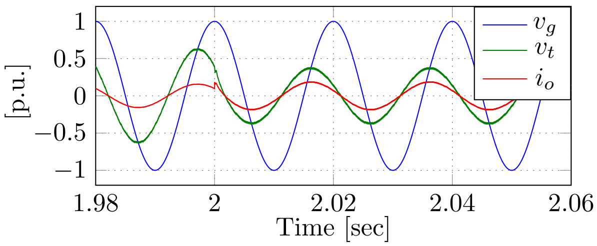

Fig. 9: Capacitive impedance emulation

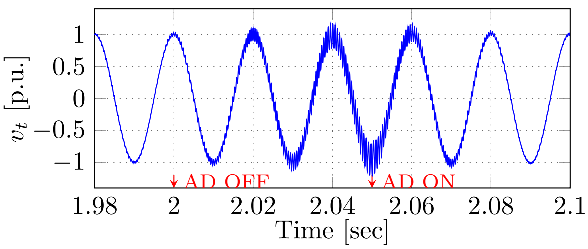

Fig. 10: Active damping

applied to show the dynamic performance of the controller. A capacitance of 40μF is emulated in series with the grid, and a similar step change in the load is applied at $t = 2$ sec and the results are shown in Fig. 9.

The effectiveness of AD technique is tested at no load, where the damping from the load side is minimal. The AD is turned off at $t = 2$ sec and re-enabled at $t = 2.05$ sec as shown in Fig. 10. From the plot, it is clear that soon as the AD gets disabled the resonance starts building up and when it is re-enabled, the resonance is damped-out.

B. Experimental Results

The proposed grid emulator is verified experimentally on a low voltage laboratory prototype. The closed-loop voltage control is implemented on TMS320F28355. The load connected to the PCC is a non-linear diode rectifier in series with an inductor on the AC side. Fig. 11a shows the steady state filter capacitor voltage with harmonic resonant controllers disabled. When the harmonic resonant controllers are enabled, the output voltage is free from 3^{rd},$5^{th}$and 7^{th} harmonics as shown in Fig. 11b. The experimental result with series resistive impedance emulation is given in Fig. 11c. The output voltage is distorted because of the harmonic voltage drop across the emulated resistor.

VI. Conclusion

This paper proposes a simple way to emulate a grid with a virtual series impedance. The control structure ensures tracking of any desired harmonic voltage. The proposed observer-based active damping technique provides enough damping to LC resonance. The performance of the grid emulator for different grid impedance was analysed in detail using time domain simulations. The experimental results provided validates the performance of the voltage controller to track harmonic voltage caused due to non-linear loads connected to the grid emulator.

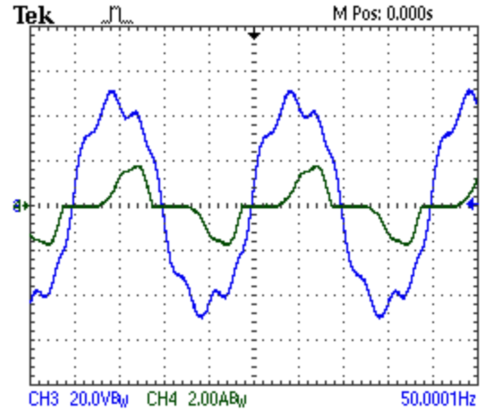

(a) Without harmonic controller

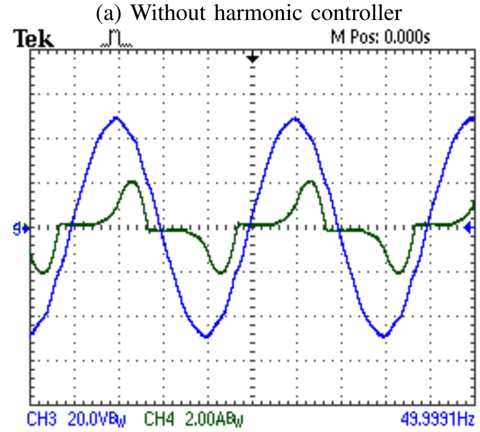

(b) With harmonic controller

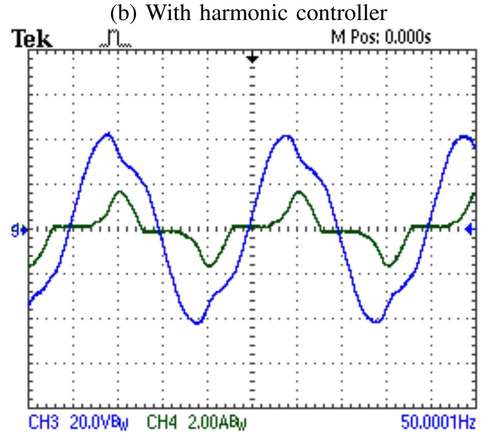

(c) Resistive emulation

Fig. 11: PCC voltage v_t (blue) and current $i_o(t)$(green); (x axis: 5 ms/div and y axis V: 20 V/div and I: 2 A/div)

References

[1] D. M. Vilathgamuwa, P. C. Loh, and Y. Li, “Protection of microgrids during utility voltage sags,” *IEEE Transactions on Industrial Electronics*, vol. 53, no. 5, pp. 1427–1436, Oct 2006.

[2] T. Midtsund, J. A. Suul, and T. Undeland, “Evaluation of current controller performance and stability for voltage source converters connected to a weak grid,” in *The 2nd International Symposium on Power Electronics for Distributed Generation Systems*, June 2010, pp. 382–388.

[3] D. Dong, B. Wen, D. Boroyevich, P. Mattavelli, and Y. Xue, “Analysis of phase-locked loop low-frequency stability in three-phase grid-connected power converters considering impedance interactions,” *IEEE Transactions on Industrial Electronics*, vol. 62, no. 1, pp. 310–321, Jan 2015.

[4] "Ieee standard for interconnection and interoperability of distributed energy resources with associated electric power systems interfaces," *IEEE Std 1547-2018 (Revision of IEEE Std 1547-2003)*, pp. 1–138, April 2018.

[5] M. Cspedes, T. Qi, and J. Sun, "Development of a grid simulator," in *2012 IEEE 13th Workshop on Control and Modeling for Power Electronics (COMPEL)*, June 2012, pp. 1–8.

[6] J. Eloy-Garcia, J. C. Vasquez, and J. M. Guerrero, "Grid simulator for power quality assessment of micro-grids," *IET Power Electronics*, vol. 6, no. 4, pp. 700–709, April 2013.

[7] B. A. Karuppaswamy, S. Gulur, and V. John, "A grid simulator to evaluate control performance of grid-connected inverters," in *2014 IEEE International Conference on Power Electronics, Drives and Energy Systems (PEDES)*, Dec 2014, pp. 1–6.

[8] X. Chen and J. Sun, "Characterization of inverter-grid interactions using a hardware-in-the-loop system test-bed," in *8th International Conference on Power Electronics - ECCE Asia*, May 2011, pp. 2180–2187.

[9] *ACS 6000 grid simulator*. [Online]. Available: https://new.abb.com/drives/medium-voltage-ac-drives/acs6000

[10] *Chroma 61800 grid simulator*. [Online]. Available: https://www.chromausa.com/product/regenerative-grid-simulator-61800/

[11] *Cinergia grid simulator*. [Online]. Available: http://www.cinergia.coop/cinergia-product/ge-grid-emulator-series

[12] X. Wang, Y. W. Li, F. Blaabjerg, and P. C. Loh, "Virtual-impedance-based control for voltage-source and current-source converters," *IEEE Transactions on Power Electronics*, vol. 30, no. 12, pp. 7019–7037, Dec 2015.

[13] K. Hatua, A. K. Jain, D. Banerjee, and V. T. Ranganathan, "Active damping of output lc filter resonance for vector-controlled vsi-fed ac motor drives," *IEEE Transactions on Industrial Electronics*, vol. 59, no. 1, pp. 334–342, Jan 2012.

[14] C. Wessels, J. Dannehl, and F. W. Fuchs, "Active damping of lcl-filter resonance based on virtual resistor for pwm rectifiers ; stability analysis with different filter parameters," in *2008 IEEE Power Electronics Specialists Conference*, June 2008, pp. 3532–3538.

[15] M. Malinowski and S. Bernet, "A simple voltage sensorless active damping scheme for three-phase pwm converters with an lcl filter," *IEEE Transactions on Industrial Electronics*, vol. 55, no. 4, pp. 1876–1880, April 2008.

[16] A. Ghoshal and V. John, "Active damping of lcl filter at low switching to resonance frequency ratio," *IET Power Electronics*, vol. 8, no. 4, pp. 574–582, 2015.

[17] V. Miskovic, V. Blasko, T. M. Jahns, A. H. C. Smith, and C. Romenesko, "Observer-based active damping of lcl resonance in grid-connected voltage source converters," *IEEE Transactions on Industry Applications*, vol. 50, no. 6, pp. 3977–3985, Nov 2014.

[18] H. W. Dommel, *Electromagnetic Transients Program: Reference Manual:(EMTP theory book)*. Bonneville Power Administration, 1986.

[19] K. N. Narayanan, L. Umananad, and S. S.

[20] X. Yuan, W. Merk, H. Stemmler, and J. Allmeling, "Stationary-frame generalized integrators for current control of active power filters with zero steady-state error for current harmonics of concern under unbalanced and distorted operating conditions," *IEEE Transactions on Industry Applications*, vol. 38, no. 2, pp. 523–532, Mar 2002.

[21] A. G. Yepes, F. D. Freijedo, J. Doval-Gandoy, . Lpez, J. Malvar, and P. Fernandez-Comesaa, "Effects of discretization methods on the performance of resonant controllers," *IEEE Transactions on Power Electronics*, vol. 25, no. 7, pp. 1692–1712, July 2010.